Structural basis for the channel function of a degraded ABC transporter, CFTR (ABCC7)

Yonghong Bai,[1,2] Min Li,[1] and Tzyh-Chang Hwang[1,2,3]

[1]Dalton Cardiovascular Research Center, [2]Department of Biological Engineering, and [3]Department of Medical Pharmacology and Physiology, University of Missouri-Columbia, Columbia, MO 65211

Cystic fibrosis transmembrane conductance regulator (CFTR) is a member of the ATP-binding cassette (ABC) transporter superfamily, but little is known about how this ion channel that harbors an uninterrupted ion permeation pathway evolves from a transporter that works by alternately exposing its substrate conduit to the two sides of the membrane. Here, we assessed reactivity of intracellularly applied thiol-specific probes with cysteine residues substituted into the 12th transmembrane segment (TM12) of CFTR. Our experimental data showing high reaction rates of substituted cysteines toward the probes, strong blocker protection of cysteines against reaction, and reaction-induced alterations in channel conductance support the idea that TM12 of CFTR contributes to the lining of the ion permeation pathway. Together with previous work, these findings raise the possibility that pore-lining elements of CFTR involve structural components resembling those that form the substrate translocation pathway of ABC transporters. In addition, comparison of reaction rates in the open and closed states of the CFTR channel leads us to propose that upon channel opening, the wide cytoplasmic vestibule tightens and the pore-lining TM12 rotates along its helical axis. This simple model for gating conformational changes in the inner pore domain of CFTR argues that the gating transition of CFTR and the transport cycle of ABC proteins share analogous conformational changes. Collectively, our data corroborate the popular hypothesis that degradation of the cytoplasmic-side gate turned an ABC transporter into the CFTR channel.

The Journal of General Physiology

INTRODUCTION

Ion channels and active transporters, two large classes of integral membrane proteins, play pivotal roles in catalyzing the translocation of ions and other substrates across biological membranes. Ion channels, when open, craft a continuous polar pathway that permits selected ions to diffuse passively across the hydrophobic barrier of phospholipid bilayers (Hille, 2001). In contrast, active transporters move substrates against their electrochemical gradient at a rate significantly lower than that of an ion channel (Artigas and Gadsby, 2003; Jayaram et al., 2008). An active transport cycle also requires an input of free energy derived from either an established concentration gradient or ATP (Gadsby, 2009). To avoid dissipation of the concentration gradient through simple diffusion, it has long been proposed that the substrate-binding site for an active transporter is forbidden to be simultaneously accessible to both sides of the membrane, namely, the alternating-access model (Jardetzky, 1966). Despite these distinct mechanisms in their functions, recent studies of members from each class reveal surprising structural similarities (Dutzler et al., 2003; Accardi and Miller, 2004). In fact, at least two families of membrane proteins, ATP-binding cassette (ABC) transporters and chloride channel (CLC) proteins, consist of both ion channels and transporters as their members (Chen and Hwang, 2008).

ABC transporters (Dawson et al., 2007; Hollenstein et al., 2007; Oldham et al., 2008; Rees et al., 2009) harness the energy of ATP binding and hydrolysis to power the movement of a broad range of substrates into (importers) or out of (exporters) cells. ABC importers, present exclusively in prokaryotes, are important for uptake of nutrients. ABC exporters, on the other hand, are found in all kingdoms of life and are involved in extrusion of, among others, a variety of endobiotics or xenobiotics. Regardless of the chemical nature of their transported substrates, the core architecture of ABC transporters, exhibiting an internal twofold or pseudo-twofold symmetry, comprises two transmembrane domains (TMDs; TMD1 and TMD2), which form the substrate translocation pathway, and two cytosolic nucleotide-binding domains (NBDs; NBD1 and NBD2) that interact with ATP. Crystallographic studies of full-length ABC proteins have provided structural evidence supporting the alternating-access hypothesis (Ward et al., 2007;

Correspondence to Tzyh-Chang Hwang: hwangt@health.missouri.edu

Abbreviations used in this paper: ABC, ATP-binding cassette; CLC, chloride channel; DTT, dithiothreitol; MTS, methanethiosulfonate; MTSACE, 2-aminocarbonylethyl MTS; MTSEA$^+$, 2-aminoethyl MTS hydrochloride; MTSES$-$, 2-sulfonatoethyl MTS; MTSET$^+$, 2-trimethylaminoethyl MTS; NBD, nucleotide-binding domain; TM, transmembrane segment; TMD, transmembrane domain.

The Rockefeller University Press $30.00
J. Gen. Physiol. Vol. 138 No. 5 495–507
www.jgp.org/cgi/doi/10.1085/jgp.201110705

Khare et al., 2009). During each transport cycle, ATP-mediated assembly and separation of the two NBDs are coupled to conformational interconversion between outward- and inward-facing configurations of the TMDs.

Phylogenetic analysis has placed the CFTR protein, defective in patients with cystic fibrosis, in the C subclass of human ABC proteins, or ABCC (Dean and Annilo, 2005). However, although many of the ABCC members are exporters that pump endogenous or xenobiotic organic anions out of the cells (Paumi et al., 2009), CFTR functions as an ATP-gated CLC (Riordan et al., 1989; Bear et al., 1992). Despite this functional distinction, it is well established that both CFTR and ABC transporters use similar molecular mechanisms at the level of NBDs; namely, ATP binding to the well-conserved motifs initiates the formation of an NBD dimer. For CFTR, this assembly of an NBD dimer is accompanied by opening of the anion-selective pore located in the TMDs (Vergani et al., 2005; Mense et al., 2006).

With respect to the TMDs, CFTR and ABC exporters conform to a "6 + 6" topological fold, with each TMD bearing six transmembrane segments (TMs) and the last TM (TM6 and TM12) in each TMD fused to an NBD. Crystal structures for three ABC exporters, including the Sav1866 multidrug exporter (Dawson and Locher, 2006, 2007), the MsbA lipid flippase exporter (Ward et al., 2007) from bacteria, and the mouse multidrug exporter P-glycoprotein, or ABCB1 (Aller et al., 2009), have been solved recently. In all these structures the two TMDs form two domain-swapped wings, each of which is composed of two TMs from one TMD and four other TMs from the partner TMD. As for the TMs that lie along the substrate translocation pathway, co-crystallization of P-glycoprotein with two different cyclic peptide inhibitors in its inward-facing configuration (Aller et al., 2009) reveals that the drug-binding site involves residues from both TM6 and TM12 (Fig. S1), a picture supported by functional studies (Loo and Clarke, 1997). On the other hand, the outward-facing structures of homodimeric SAV1866 (Dawson and Locher, 2006) and MsbA (Ward et al., 2007) also lead the authors to propose that their substrate translocation pathway is partly formed by TM6 from each TMD (Fig. S1). Thus, for ABC exporters the molecular architecture of the TMDs may be evolutionarily conserved through millions of years. Interestingly, numerous studies indeed have identified TM6 as a pore-lining domain for CFTR (McDonough et al., 1994; Smith et al., 2001; Alexander et al., 2009; Bai et al., 2010; El Hiani and Linsdell, 2010).

However, CFTR and ABC exporters belong to two distinct functional subtypes (channels vs. transporters), which dictate dissimilar mechanistic functions of their TMDs. In CFTR, ATP-induced dimerization of the NBDs opens the channel pore, whereas in ABC exporters, the formation of the NBD dimer converts the TMDs to an outward-facing conformation with an obliterated internal entrance. To reconcile the functionally distinct roles of the substrate–translocation pathways for CFTR and ABC transporters, it has been hypothesized (Chen and Hwang, 2008; Jordan et al., 2008; Gadsby, 2009) that CFTR evolves from a primordial ABC exporter by simply degrading the cytoplasmic gate. This hypothesis, however appealing, is short of experimental evidence. In fact, recent studies (Ward et al., 2007; El Hiani and Linsdell, 2010; Qian et al., 2011) have suggested that CFTR channel gating involves a gated access of the pore from the cell interior.

Here, guided by the twofold symmetrical structures of ABC exporters, we used the cysteine-scanning method to investigate the role of TM12 of CFTR in ion permeation and gating motion. Our collective findings suggest a structural basis for CFTR to function as a degraded ABC exporter. First, our data indicate that this TM assumes an α-helical structure and lines the hydrophilic ion permeation pathway. Thus, both TM6 and TM12 of CFTR, the two TMs that are related by an internal pseudo-twofold symmetry, contribute to the formation of the ion permeation pathway, a theme that is in agreement with the framework of the substrate translocation pathway observed in ABC exporters. Second, the reactivity profile determined with intracellular probes indicates the presence of a large aqueous internal vestibule in both the open and closed states of CFTR, consistent with the idea that evolutionary removal of the cytoplasmic barrier in an ABC exporter confers CFTR the channel function. Finally, the state-dependent reactivity change is in line with a simple model in which TM12 of CFTR undergoes a rotational movement and the cytoplasmic end of the ion permeation pathway tightens during channel opening. These conformational changes bear resemblances to those proposed for ABC export cycles.

MATERIALS AND METHODS

Molecular biology

The source and property of the cysless–CFTR construct have been described previously (Bai et al., 2010). Site-directed mutations were generated by PCR and confirmed by sequencing. Chinese hamster ovary cells were transfected with channel constructs and a green fluorescent protein cDNA construct and were incubated for 2–4 d before recording. Procedures for mutagenesis, cell culture, and transfection have been described previously (Bai et al., 2010).

Electrophysiology

Macroscopic and microscopic current recordings were performed on excised inside-out membrane patches as described previously (Bai et al., 2010). Pipette solution contained (in mM): 140 NMDG-Cl, 2 $MgCl_2$, 5 $CaCl_2$, and 10 HEPES, adjusted to pH 7.4 with NMDG. Intracellular solution (perfusion solution) contained (in mM): 150 NMDG-Cl, 10 EGTA, 10 HEPES, 8 Tris, and 2 $MgCl_2$, adjusted to pH 7.4 with NMDG. Intracellular solutions were rapidly (~30 ms) exchanged using SF-77B solution exchange system. Program-controlled solution exchange was used for repeated short

applications (Figs. 5 and 6). Unless noted otherwise, all currents were recorded at −50 mV membrane potential. Data were continuously acquired with a patch-clamp amplifier (EPC10; HEKA), filtered at 100 Hz using an eight-pole Bessel filter, and digitized online at 500 Hz. Single-channel amplitude (Fig. 4) was estimated by multi-peak Gaussian fittings of the all-point amplitude histogram of continuous (>30-s) recordings.

Chemical modification

To minimize spontaneous oxidation of the introduced cysteines, channels were pretreated with 10 mM dithiothreitol (DTT) during the activation by PKA and ATP, which usually takes 2–5 min, before modification experiments. All methanethiosulfonate (MTS) reagents were purchased from Toronto Research Chemicals. Hydrophilic reagents were prepared as 100-mM stock solutions in ddH_2O, whereas the hydrophobic reagent, Texas red 2-aminoethyl MTS hydrochloride ($MTSEA^+$), was solved in DMSO to make 10-mM stock solutions. Aliquots of the stock solution were thawed into the perfusion solution and used immediately. The working concentration of MTS was lowered to 1 µM to measure the highest modification rate and raised to 3 mM to measure the lowest modification rate. Modification time constants (τ) were obtained by fitting continuous (Fig. 2, A and B) or stepwise (Figs. 5 and 6) current relaxation time courses with single-exponential functions. Second-order modification rate constants (κ_{MTS}) were calculated according to $\kappa_{MTS} = 1 / (\tau \times [MTS])$, where [MTS] was the working concentration of MTS.

For the analysis of blocker protection effects, an ideal result to show complete protection would be that when channels are all in the blocked state, modification is prohibited. But this experiment is not technically feasible because under the highest concentration (200 µM) of the hydrophobic blocker glibenclamide that can be achieved, the fraction of current blockade (f_b) is ∼80%. However, if we assume that in the presence of the blocker there are two populations of channels, blocked and unblocked, the modification rate for blocked channels can be estimated as described previously (del Camino et al., 2000). The modification rate constant in the presence of the blocker (κ_{MTS}) would be a weighted average between that of blocked and unblocked channels: $\kappa_{MTS} = f_b \times \kappa_{MTS\text{-}b} + (1 - f_b) \times \kappa_{MTS\text{-}ub}$, where $\kappa_{MTS\text{-}b}$ and $\kappa_{MTS\text{-}ub}$ are the modification rate constants for blocked and unblocked channels, respectively. Solving the equation yields that $\kappa_{MTS\text{-}b} = [1/f_b] \times \kappa_{MTS} - [(1 - f_b)/f_b] \times \kappa_{MTS\text{-}ub}$. By comparing the values of $\kappa_{MTS\text{-}b}$ and $\kappa_{MTS\text{-}ub}$, we can obtain the relative modification rate constant of blocked channels to that of unblocked ones (R; Fig. 4 C): $R = \kappa_{MTS\text{-}b}/\kappa_{MTS\text{-}ub}$. If R = 0, it means that the blocker completely protects the cysteine from modification. If R = 1, it means that the blocker does not have any effect on modification. The smaller the value of R is, the stronger the protection effect.

To measure the reaction rate of cysteines with MTS reagents in the absence of ATP (Fig. 5), we have adopted an experimental protocol similar to what has been developed by Yellen's group (Liu et al., 1997) and Swartz's group (Li et al., 2010). Our protocol contains 12 repeats of programmed solution exchange, with each repeat containing a 3-s application of ATP followed by an 8-s washout, and a 3-s application of MTS reagents followed by a 2-s washout. Because PKA is not present during this protocol, we have taken several precautions to ensure that current rundown caused by dephosphorylation is miniscule. First, the overall duration for the entire protocol is comparable to that of the measurement for MTS modification in the presence of ATP. As we observed negligible current rundown caused by dephosphorylation in our measurement of MTS modification in the presence of ATP, we reckon that this effect of rundown should also be minimal for MTS modification in the absence of ATP. Second, we applied two 3-s ATP pulses, each followed by an 8-s washout, and compared the current induced by these first two pulse applications of ATP to ensure no significant spontaneous current rundown before carrying out the protocol for MTS modification. Third, in several cases, we were able to observe a steady level of current during the last several applications of ATP, indicating a completion of the modification and an absence of spontaneous current rundown after MTS modification.

Despite these precautious measures, the protocol does not allow direct measurements of the modification rate for closed channels for two reasons. First, it is known that CFTR assumes a low but significant opening rate even in the complete absence of ATP. Second, although an 8-s washout time is sufficient for closing of ∼95% of the ATP-opened channels, a small fraction of the channels remains in the open state when MTS reagents are applied. How this technical imperfection affects our data and why it does not alter our conclusions are described in the online supplemental material.

Online supplemental material

Fig. S1 shows similar overall TMD architectures in three different ABC exporters. Fig. S2 demonstrates that the positively charged 2-trimethylaminoethyl MTS ($MTSET^+$) adduct in TM12 enhances the effect of an anionic blocker, glibenclamide. Fig. S3 is a representative trace that illustrates protection of a substituted cysteine in TM12 by glibenclamide. Fig. S4 demonstrates modification of cysless/T1142C channels in the presence of ATP plus pyrophosphate. Fig. S5 shows the data for modification rates in the cysless/E1371Q background. Fig. S6 depicts a representative trace showing modification of cysless/W1145C channels in the absence of ATP. Fig. S7 is a plot showing that the differences between the modification rate in the presence of ATP and that in the absence of ATP are qualitatively reliable indicators of the true differences between the modification rate in open channels and that in closed channels. Tables S1 and S2 summarize the accessibility of individual cysteines in TM6 and TM12, respectively, from our study as well as from other reports. The supplemental text (Section 1) details the similarities and discrepancies in these cysteine-scanning results for TM6 and TM12. Section 2 provides semi-quantitative analyses of the relationship between MTS modification rates for the open and closed states and those measured in the presence and absence of ATP.

RESULTS

Cysteine scanning of TM12 identifies intracellular reactive positions

We introduced cysteine residues individually throughout TM12 (1129–1150) of CFTR and characterized their sensitivity to the water-soluble, negatively charged thiol-specific 2-sulfonatoethyl MTS ($MTSES^-$). For 8 of the 22 cysteine-substituted CFTR channels, the ATP-elicited chloride current was markedly decreased upon the application of $MTSES^-$ to the intracellular side of inside-out membrane patches (Fig. 1, A and C). This effect persisted after removal of $MTSES^-$, indicating covalent modifications of the introduced cysteines. In contrast, the function of the remaining mutant channels appeared unaltered during 1-min exposure to 1 mM $MTSES^-$ (Fig. 1, B and C). We found an abrupt cessation of reactivity around the middle of TM12 (Fig. 1 C, dotted line). Consequently, the apparent reactive sites all reside in the cytoplasmic part of TM12. This result is similar to our previous observation with TM6 (Bai et al., 2010) and validates the

notion that the CFTR channel is not permeable to the bulky MTS reagents (~6 × 10 Å) (Smith et al., 2001).

We next measured the time constant of the single-exponential current relaxation upon $MTSES^-$ treatment and calculated the second-order reaction rate constant (Fig. 2). The reaction rate for positions 1141, 1145, and 1148 is exceedingly high and close to that for $MTSES^-$ reaction with free thiols in the bulk solution (Karlin and Akabas, 1998) (Fig. 2, B and C), suggesting that these three positions are well exposed to a water-accessible area. In contrast, modification of cysteines at positions immediately adjacent to or one amino acid residue apart from these highly reactive sites (Fig. 2, A and C) is either relatively slow (1140, 1142, 1144, 1147, and 1150) or undetectable (1143, 1146, and 1149). The low reactivity could be a result of either limited water accessibility or unfavorable microenvironment (e.g., nearby charges) for the reaction of $MTSES^-$ with thiolates. However, the overall reactivity pattern exhibits a helical periodicity (Fig. 2 D) and is consistent with a simplified model in which the internal part of TM12 assumes a secondary structure of an α helix, and the helix is arranged in such a manner that three side chains on one face of the helix are freely exposed to a polar environment, whereas the remaining ones are partially or completely buried in a more hydrophobic part of the CFTR protein.

The cytoplasmic part of TM12 contributes to the lining of the anion permeation pathway

Notably, our initial cysteine-scanning data define a water-accessible cytoplasmic region (1140–1150) of TM12. It remains questionable, however, whether this region is part of the ion conduction pathway of the CFTR channel, because the loss of channel function after $MTSES^-$ modification may be attributed to two equally possible explanations: a reduced chance that channels stay open or hindered chloride flow when channels are open. Indeed, cysteine residues engineered in the voltage-sensing domain of K_v channels and the gating ring of cyclic nucleotide–gated channels can be readily modified by thiol reagents, but these regions, rather than lining the aqueous ion pathways, are gating domains that modulate channel open probability (Larsson et al., 1996; Johnson and Zagotta, 2005). To identify the cause of the macroscopic current decrease upon $MTSES^-$ exposure, we took a close inspection of the current recordings and found that for $MTSES^-$-modified channels, the current decay upon washout of ATP followed a smooth path (Fig. 2, A and B, bottom traces II), where closures of individual channels cannot be discerned. Because the current amplitude of a single-channel opening before modification can be readily resolved (Fig. 2, A and B, bottom traces I), we infer that $MTSES^-$ modification drastically reduces the single-channel current amplitude by leaving a negatively charged adduct along the anion permeation pathway.

Conversely, a cationic adduct along the anion pathway may exert favorable electrostatic influence on anion passage and thereby increase the unitary current amplitude. The most likely positions for this effect to take place would be those that show the highest reaction rate for $MTSES^-$, as they are presumably widely exposed.

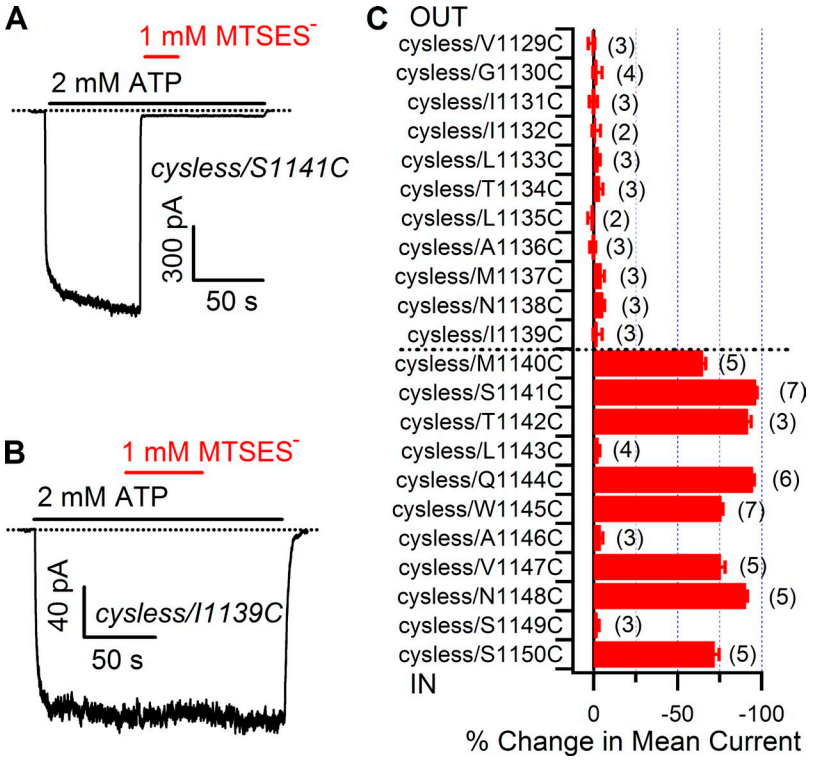

Figure 1. Cysteine scanning of TM12 of CFTR using intracellularly applied $MTSES^-$ reagents defines a cytoplasmic water-accessible region. (A) Current recorded at −50 mV in inside-out membrane patches containing thousands of cysless/S1141C-CFTR channels. Application of a saturating concentration of ATP (black lines and labels) elicited chloride currents (downward deflections). Upon intracellular $MTSES^-$ treatment (red lines and labels), the ATP-induced current decreased. Dotted line denotes the baseline. (B) Representative current recording of cysless/I1139C-CFTR channels using a similar experimental protocol as in A. Channel activity is not substantially altered by $MTSES^-$ treatment. (C) Summary of the percentage change in macroscopic current amplitude after the intracellular application of $MTSES^-$ for each cysteine-substituted channel. The dotted line marks the position beyond which no reactivity toward the cytoplasmically applied $MTSES^-$ was observed. The number near each bar marks the number of patches. Data points in this and all other figures are mean ± SEM.

Fig. 3 shows representative results from single-channel recordings. We observed that for cysteines at two cytoplasmic positions, 1145 and 1148, modification by the positively charged $MTSET^+$ increased the single-channel current amplitude (Fig. 3, A and B). Similar measurements at different membrane voltages confirmed these increases in unitary conductance. However, $MTSET^+$ modification of the cysteine at a deep position, 1141, reduced the single-channel conductance (Fig. 3 C). One plausible explanation for this aberration is that around this deep position, the ion pathway is not wide enough to accommodate the bulky $MTSET^+$ adduct without sterically obstructing ion flow. Consistent with this idea, the S1141C-CFTR channel, when modified by 2-aminocarbonylethyl MTS (MTSACE), a similarly sized but neutral reagent, also displayed a smaller single-channel current amplitude (Fig. 3 D). Overall, our observations that charged and uncharged MTS adducts at TM12 alter channel conductance suggest that the polar environment inferred from rapid $MTSES^-$ modification rates is indeed the aqueous ion permeation pathway. Thus, we conclude that the cytoplasmic part of TM12 contributes to the formation of the inner pore domain of the CFTR channel.

The substrates for many members of the ABCC subfamily to which the CFTR channel belongs are large organic anions. It is therefore not surprising that many large anions, for example, the sulfonylurea glibenclamide (Sheppard and Robinson, 1997; Zhou et al., 2002), have been characterized as channel blockers that bind within the ion permeation pathway and sterically obstruct chloride flow (Sheppard and Welsh, 1999; Chen and Hwang, 2008). This channel-blocking mechanism is consistent with our finding that increasing the electropositivity of the inner pore domain by the deposition of $MTSET^+$ adducts not only accelerates the chloride flow but also enhances the potency of the anionic blocker glibenclamide (Fig. S2). Thus, for channels with cysteines substituted into any of the three highly reactive positions (1141, 1145, and 1148) that presumably face the permeation pathway, the degree of block under the same concentration of glibenclamide is enhanced after $MTSET^+$ treatment.

Spurred by this experimental observation, we next sought to investigate the possibility that glibenclamide binding would alter the accessibility of the engineered cysteines. We applied $MTSES^-$ in the continuous presence of 200 µM glibenclamide and measured its modification

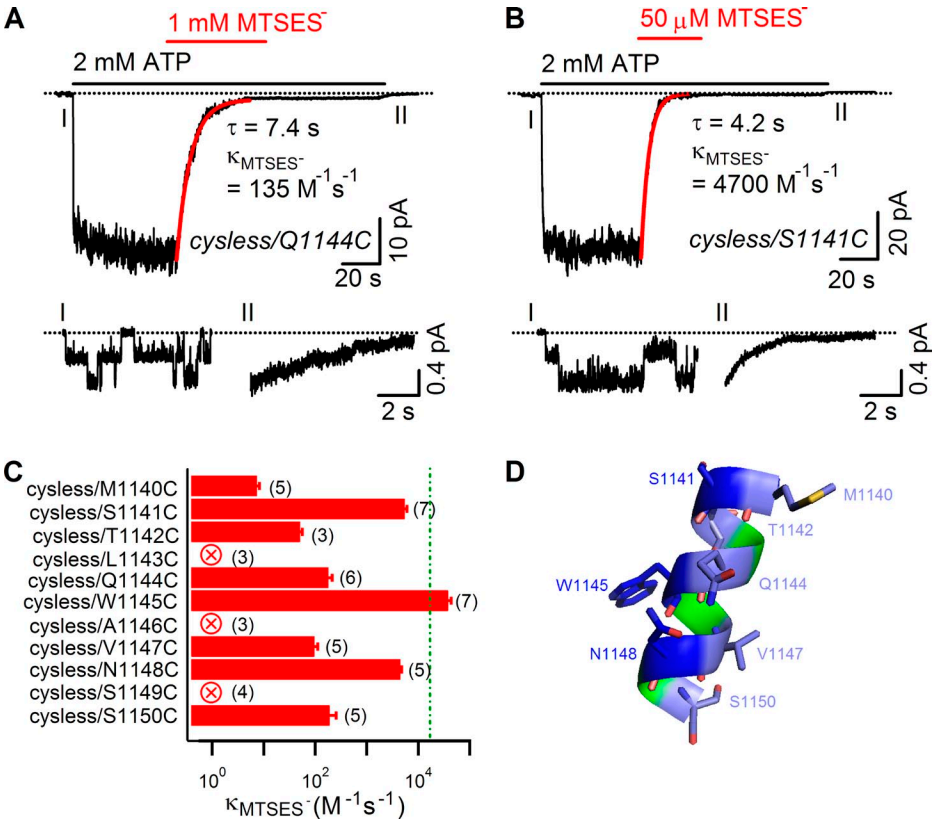

Figure 2. Measurements of the second-order reaction rate reveal that TM12 assumes an α-helical structure. (A and B) Measurements of the second-order reaction rate constant (κ_{MTSES^-}) of $MTSES^-$ modification in the presence of 2 mM ATP for cysless/Q1144C (A) and cysless/S1141C (B). Single-exponential fitting (red line) of the current relaxation in response to $MTSES^-$ treatment yields the modification time constant (τ), the reciprocal of which divided by the concentration of $MTSES^-$ gives κ_{MTSES^-}. (Bottom traces I and II) Expanded view of portions of top traces (as marked) to show that the single-channel amplitude is diminished after $MTSES^-$ exposure. (C) Summary of the modification rate constant at each position of the cytoplasmic half of TM12. Note that reaction rate at positions 1141, 1145, and 1148 approximates that of $MTSES^-$ with free thiols (green line). Crossed circles mark cysteine-substituted channels whose function was not significantly altered by the treatment of $MTSES^-$. The number near each bar represents the number of patches. (D) Helical structure of the cytoplasmic half of TM12 inferred from C. Blue, positions where introduced cysteines were readily accessible to $MTSES^-$; light blue, positions where cysteines were less accessible; green, positions where no accessibility was observed.

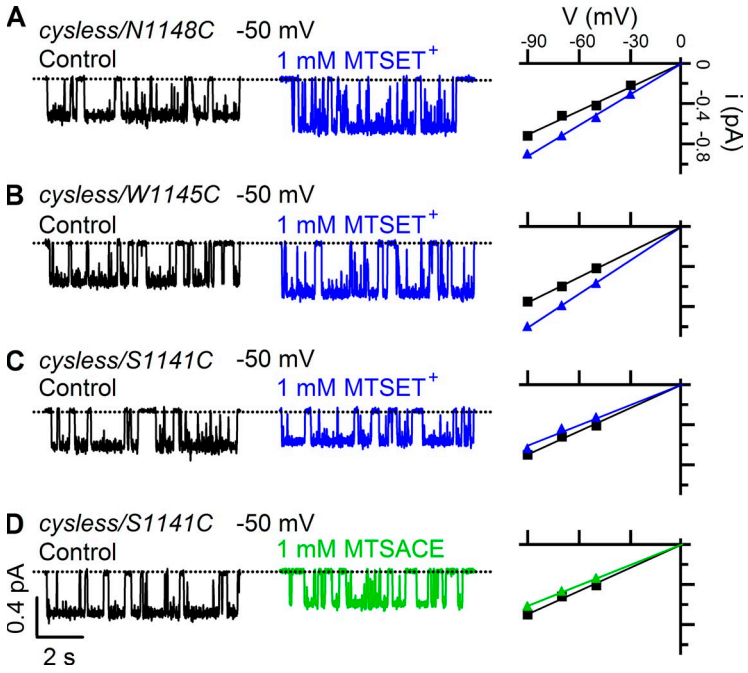

Figure 3. Covalent modifications by MTS reagents alter the single-channel conductance. (A and B) Single-channel recordings at −50 mV show that application of $MTSET^+$ increases unitary current amplitudes for cysless/N1148C (A) or cysless/W1145C (B). Linear fits to single-channel current measurements at different voltages yield unitary conductance values for cysless/N1148C (A) of 7.1 pS before (black) and 9.2 pS after (blue) $MTSET^+$ treatment, for cysless/W1145C (B) of 7.6 pS before (black) and 10.1 pS after (blue) $MTSET^+$ treatment. (C and D) Single-channel recordings show that the unitary current amplitude decreases after $MTSET^+$ (C; blue) or MTSACE (D; green) exposure for cysless/S1141C. Linear fits to single-channel current measurements at different voltages yield unitary conductance values for cysless/S1141C of 7.0 pS before (C and D; black) and 6.1 pS after both $MTSET^+$ (C; blue) and MTSACE (D; green) treatment. Each data point is the average of three to six patches. Symbols are larger than SEM.

rate constant (Fig. 4 A, orange line). Because the fraction of block under this concentration is less than one, the apparent rate constant reflects a weighted average between those for blocked and unblocked channels. After the modification is reversed by the reducing reagent DTT, we applied $MTSES^-$ in the absence of glibenclamide (Fig. 4 A, red line) in the same patch and again measured its modification rate constant, which represents that of unblocked channels. Comparing the two rate constants and correcting for the fraction of block, we computed the relative rate of blocked channels to unblocked ones. Our results show that for blocker-bound channels, modification rate constants are over twenty-fold slower for cysteines at positions 1141 and 1145 (Fig. 4, B and C), indicating that the bound blocker strongly protects these cysteines against modification. For the more cytoplasmic position, 1148, cysteine modification rate is reduced by less than fourfold (Figs. 4 C and S3). This is probably because the inner pore is sufficiently wide toward its cytoplasmic end to accommodate both glibenclamide and $MTSES^-$. Collectively, these data showing the enhanced channel blockade owing to the positively charged MTS adduct and the restricted cysteine accessibility upon pore blockade provide additional

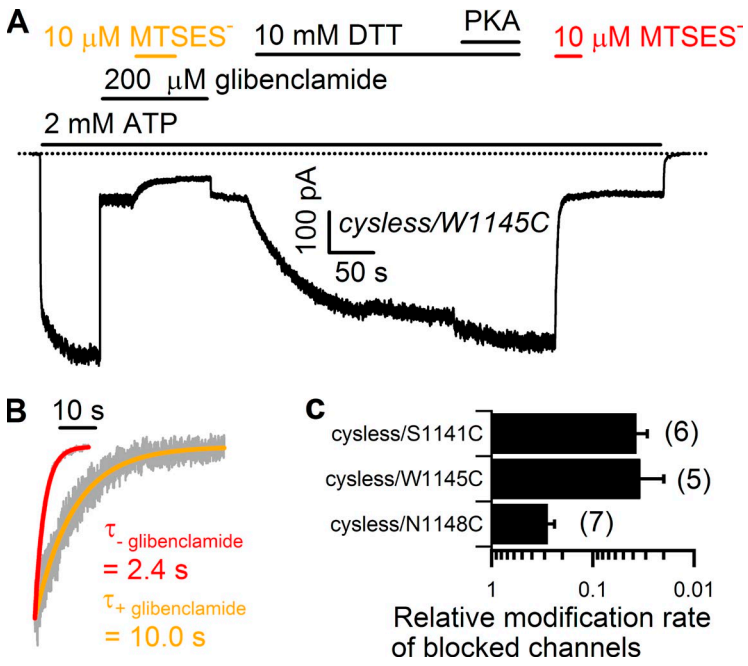

Figure 4. The blocker glibenclamide protects engineered cysteine residues from modification by $MTSES^-$. (A) In an inside-out patch containing thousands of cysless/W1145C-CFTR channels, $MTSES^-$ was first (indicated by orange lines) applied in the presence of 200 μM glibenclamide (yielding 77% steady-state blockade), and then (red lines) in the absence of glibenclamide after the chemical modification was reversed by the reducing reagent, DTT. (B) Comparison of modification time courses with or without glibenclamide. Portions of the current trace from A were normalized in current amplitude and fitted with single-exponential functions, yielding the modification time constant (τ), as indicated in the figure. This comparison shows that modification rate with glibenclamide (orange) is 24% of that without glibenclamide (red). Thus, the presence of glibenclamide almost completely protects the cysteine against modification, given that the fraction of block is 77%. (C) The bars originating at 1 and ending at a value of <1 on the logarithmic axis correspond to the decrease in the modification rate produced by the blocker glibenclamide. The relative modification rate of blocked channels compared with unblocked ones was corrected for the fraction of block (see Materials and methods).

support for the idea that the cytoplasmic part of TM12 lines the ion permeation pathway.

Accessibility of cytoplasmically applied MTSES⁻ in closed CFTR channels

In an attempt to understand how the CFTR channel pore is gated, we further tested reactivity of $MTSES^-$ with cysteines at the pore-lining TM12 in the absence of ATP. We measured modification rate constants by plotting the stepwise current decay upon repeated brief (3-s) $MTSES^-$ treatments after an 8-s washout of ATP (Fig. 5 A). The differences we observed between the rate constants measured with this protocol (Fig. 5 A) and those measured in the presence of ATP (Fig. 2 C) presumably reflect the alterations of the accessibility of the cysteines as a result of gating conformational changes in the ion permeation pathway. It is notable that, because channel open probability is neither unity in the presence of ATP nor zero after an 8-s washout of ATP, the differences between the modification rate with ATP and that without ATP tend to slightly underestimate the true differences between the modification rate of cysteines in open channels and that in closed channels, but our data are qualitatively reliable in portending whether there are such differences and the nature of such differences (see supplemental text, Section 2, for details). We found that cysteines at positions 1140, 1144, and 1148 can be modified by $MTSES^-$ more rapidly in the absence of ATP (Fig. 5, B and D) than in the presence of ATP, suggesting that these residues are exposed to a more hydrophilic environment in closed channels. On the other hand, modification rates for cysteines at positions 1141, 1142, 1145, 1147, and 1150 are relatively slower in the absence of ATP (Figs. 5 C and D, and S6), suggesting that the amino acid side chains at these positions moved to a more hydrophobic part of the protein in the closed state. One important feature of the reactivity pattern is that there is no abrupt cessation of reactivity in the absence of ATP along the cytoplasmic part (1140–1150) of TM12. This result is inconsistent with the idea that access of the channel pore to the cell interior is occluded by a physical gate toward the cytoplasmic end, as seen in the voltage-gated K^+ channels (Liu et al., 1997). Thus, we propose that in a closed channel, the ion permeation pathway

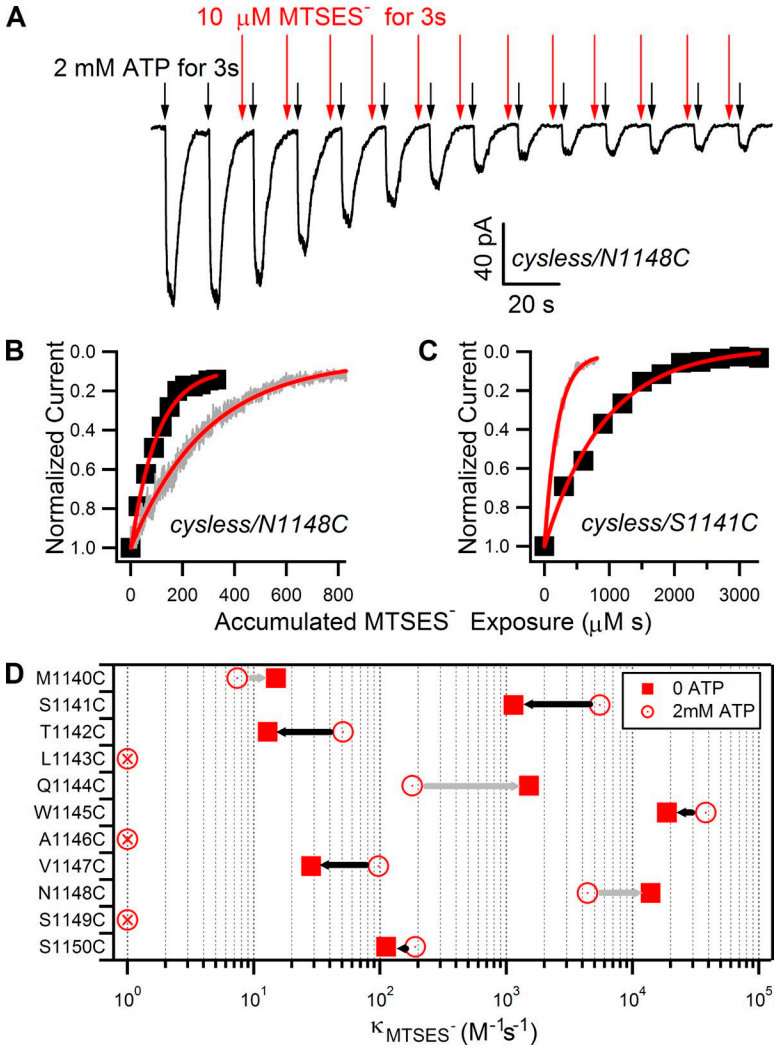

Figure 5. Comparisons of the modification rate constant in the presence or absence of ATP suggest that there is no cytoplasmic-side gate in the CFTR channel. (A) A representative experiment for measuring the modification rate in the absence of ATP. Macroscopic CFTR currents elicited by applications (black arrows) of 2 mM ATP were gradually decreased upon each short application (red arrows) of $MTSES^-$ until the current level reached a steady state. (B and C) The ordinate shows the normalized current decay induced by $MTSES^-$ modification in the presence (continuous traces) or absence (closed squares) of ATP fitted into single-exponential functions (red lines). The abscissa shows accumulated $MTSES^-$ exposure (the concentration of $MTSES^-$ times the duration of the application). Note that the modification is faster in the presence of ATP than in the absence of ATP for cysless/N1148C-CFTR channels (B), whereas it is slower in the presence of ATP than in the absence of ATP for cysless/S1141C-CFTR channels (C). (D) Summary of second-order modification rate constants (κ_{MTSES^-}) with (open circles) or without (closed squares) ATP on a logarithmic scale. Black arrows connecting the two symbols indicate that κ_{MTSES^-} with ATP is larger than that without ATP, whereas gray arrows indicate that κ_{MTSES^-} with ATP is smaller than that without ATP. Crossed circles mark cysteine-substituted channels whose function was not significantly altered by the treatment of $MTSES^-$ either with or without ATP. Each data point is the average of four to seven patches. Symbols are larger than SEM.

is freely accessible to the cell interior and the gate of the CFTR pore is located at a more extracellular end of TM12, resembling the inward-facing configuration of an ABC exporter (Ward et al., 2007; Aller et al., 2009). However, the opposite directions of accessibility change for adjacent cysteines throughout the cytoplasmic part of TM12 suggest that the cytoplasmic part does undergo certain conformational rearrangements during the channel-gating process. The simplest model based on these data is that the gating conformational change involves a modest rotation in the counterclockwise direction when viewed from the intracellular side. According to this model, for instance, upon channel opening, residue 1144 would rotate toward a more hydrophilic environment and therefore can be more readily modified by $MTSES^-$, whereas residue 1145 would rotate toward a more hydrophobic environment and become more difficult to be accessed.

State-dependent accessibility of the inner pore domain to a larger MTS reagent

Thus far, our data have shown that the inner pore domain is not controlled by a cytoplasmic gate and assumes a wide vestibule structure, as this region is readily accessible to sizable intracellular compounds, such as $MTSES^-$ and glibenclamide. To further gauge the dimension of the cytoplasmic opening, we assessed the reactivity of cysteines at TM12 to a monstrous MTS reagent, Texas red $MTSEA^+$ (which has a head group of ~13 Å) (del Camino and Yellen, 2001; Li et al., 2010), with or without 2 mM ATP (Fig. 6). We found that the modification rate measured in the absence of ATP is higher than that with ATP for the cysteine introduced at either the deeper position 1141 (Fig. 6, A–C) or the more cytoplasmic position 1148 (Fig. 6 C), suggesting that both positions in a closed channel are more exposed to the bulky Texas red $MTSEA^+$ compared with those in an open channel. Similar results were obtained for positions 344 (deep in the pore) and 348 (close to the cytoplasmic end) in TM6 (Fig. 6 C), another pore-lining TM of CFTR. These results are in stark contrast to the pattern seen with $MTSES^-$ modification (Fig. 5 D), which without ATP is slower for position 1141 and faster for position 1148 than that with ATP. Thus, although the alterations in the modification rate of the smaller $MTSES^-$ can be explained by a simple helical rotation of TM12, the increase in the modification rate of the larger Texas red $MTSEA^+$ upon channel closure suggests a dilation of the inner pore domain. Repulsion against the positive charge of Texas red $MTSEA^+$ in an open channel is not likely the explanation for this effect, as

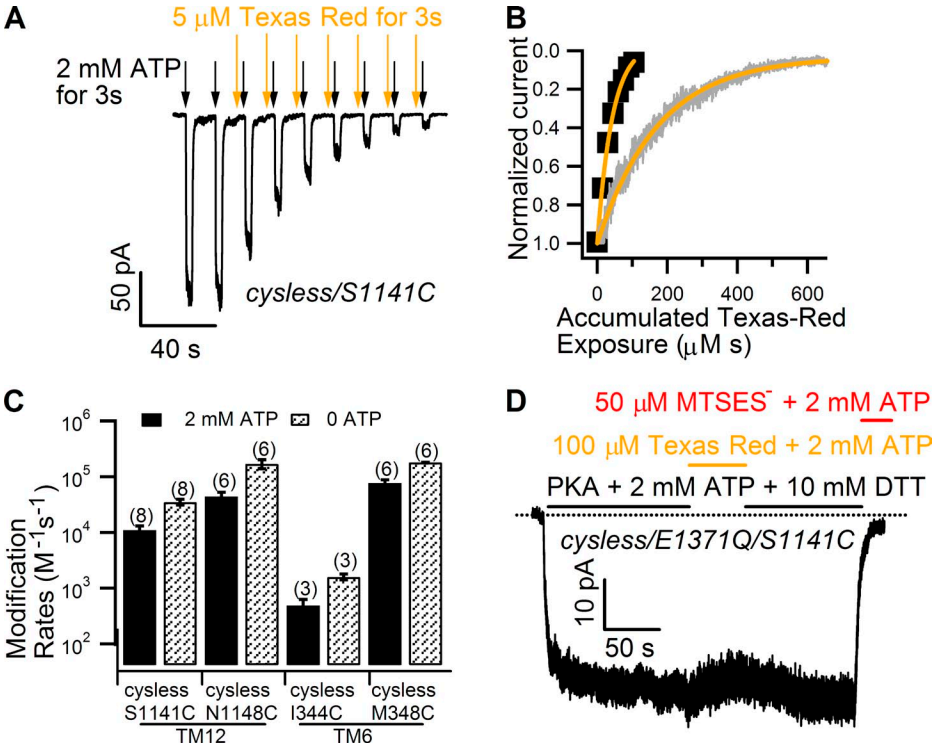

Figure 6. State-dependent modifications of a larger MTS reagent, Texas red $MTSEA^+$, suggest that the size of the inner pore entrance in the open state is smaller than that in the closed state. (A) Chemical modification of cysless/S1141C-CFTR channels by Texas red $MTSEA^+$ (orange arrows) without ATP. (B) Normalized current decay produced by Texas red $MTSEA^+$ with (continuous traces) or without (closed squares) ATP. Single-exponential fits (orange lines) yield the modification time constant (τ). Note that modification by Texas red $MTSEA^+$ without ATP is faster than that with ATP. (C) Second-order rate constants (κ_{MTSES^-}) of Texas red $MTSEA^+$ modification for cysless/S1141C-, cysless/N1148C-, cysless/I344C-, and cysless/M348C-CFTR channels. Positions 1141, 1148, 344, and 348 are located at the cytoplasmic and deep positions of TM12 and TM6, respectively. They are exposed to the watery pore as inferred from the observation that cysteines at these positions are rapidly modified by $MTSES^-$. Note that modification by Texas red $MTSEA^+$ without ATP is faster than that with ATP for all four mutant channels. (D) Channel activity is minimally altered after the prolonged (~1-min) treatment of 100 μM Texas red $MTSEA^+$, but immediately diminished upon exposure to 50 μM $MTSES^-$. Given that the E1371Q mutant channel has an open probability of near unity in the presence of ATP, this result suggests that 1141C is readily accessible to $MTSES^-$ but not to Texas red $MTSEA^+$ in an open channel. Similar results were observed for cysteines substituted into positions 1148, 344, and 348 under the E1371Q background. Each experiment was repeated in three to six patches.

$MTSET^+$ can readily react with cysteines at both TM12 (Fig. S2) and TM6 (Bai et al., 2010). Of note, given that in the presence of 2 mM ATP the open probability of the CFTR channel is less than unity, the Texas red $MTSEA^+$ modification rate measured in the presence of ATP (Fig. 6, B and C) likely overestimates the rate for the open state if the modification actually occurred only in the closed state. To better assess the modification rate of an open channel, we introduced an additional E1371Q mutation, which abolishes ATP hydrolysis and thereby confers an open probability of ∼1 on the CFTR channel. Under the E1371Q background, $MTSES^-$ readily modified 1141C resulting in a decrease of current (Fig. 6 D, red line), but Texas red $MTSEA^+$ did not react with 1141C because it neither substantially decreased the macroscopic current (Fig. 6 D, orange line) nor prevented 1141C from subsequent modification by $MTSES^-$. This result suggests that 1141C is accessible to cytoplasmic $MTSES^-$ but not Texas red $MTSEA^+$ in the open state. Similar results were also observed for positions 1148, 344, and 348. Thus, the cytoplasmic entrance of the pore in the open state is paradoxically smaller than that in the closed state.

DISCUSSION

Identifying the molecular compositions of the ion permeation pathway is central to our understanding of the structure and function of ion channels. Overall, results presented in this study provide compelling evidence supporting the idea that TM12 of the CFTR CLC contributes to the lining of the inner pore domain. First, the introduced cysteines at the cytoplasmic half of this TM can readily react with sulfhydryl reagent $MTSES^-$ resulting in a decrease of the single-channel amplitude (Fig. 1); the fact that at three positions (1141, 1145, and 1148) the reaction rate approximates that of $MTSES^-$ reaction with free thiols (Fig. 2) further suggests that part of this region of the pore is fairly wide and therefore may be considered as a vestibule that is capable of accommodating many water molecules. Second, introducing positively charged adducts at two positions (1145 and 1148) can increase the single-channel amplitude (Fig. 3), a result that is not expected to take place should these two residues reside in a narrow section of the pore. Third, a sizable blocker, glibenclamide, can bind within this region to physically occlude engineered sulfhydryls, preventing the thiol reagents from reaching them (Fig. 4). Furthermore, the overall reactivity pattern for the cytoplasmic half of TM12 displays a helical periodicity similar to our previous observation with TM6 (Fig. 2). Demonstrating that both TM6 (Bai et al., 2010) and TM12 assume a helical structure and line the chloride permeation pathway bears an important implication in regard to the evolutionary relationship between CFTR and ABC transporters, as emerging crystal structures of ABC exporters (Dawson and Locher, 2006, 2007; Ward et al., 2007; Aller et al., 2009) reveal a consistent architecture in which each TMD encompasses six transmembrane α helices, and both TM6 and TM12 contribute to the lining of the substrate translocation pathway (Fig. S1). Thus, CFTR exploits these evolutionarily conserved structural elements of the TMDs to enact the function of a gated pore.

Modification of cysteines substituted into TM12 of CFTR was also detected in a recent report from Linsdell's group (Qian et al., 2011). There is a general consensus (17 out of 19 positions that both studies have assessed) about which positions of TM12 are apparently reactive and which are not. However, although they detected reactivity in N1138C and S1149C, we found that these sites appear nonreactive. Furthermore, there are considerable differences in the second-order reaction rate constants of cysteine modification. For positions 1140–1142, reaction rates of $MTSES^-$ averaged ∼1,700, 3,000, and 3,100 $M^{-1}s^{-1}$ in their study, but averaged 7, 5,500, and 51 $M^{-1}s^{-1}$ in our own. These qualitative and quantitative discrepancies (Tables S1 and S2, and supplemental text, Section 1) were also found in cysteine-scanning studies of TM6. Although the exact reason for these disparate results seems elusive to us, several differences in the experimental design potentially contribute. First, the membrane potential under which reaction rates are measured is different (0 mV in Linsdell's studies vs. −50 mV in ours). This difference in membrane potential might explain that in some cases the modification rate of the negatively charged $MTSES^-$ reported by Linsdell's group is twofold slower than ours, but it still does not explain why in some cases their rate is over 200-fold faster. Second, our experiments were performed in a system with a constant perfusion to the membrane patch, which ensures a fast and complete solution change. We strive to present our raw data with a complete time course of the experiment. This will include the results of washout of MTS reagents as well as ATP, so that any change of the baseline can be discerned. Third, whereas our studies measured reactivity in the presence of ATP, Linsdell's group assessed reactivity in the presence of ATP, PKA, and pyrophosphate, which is presumed to maximize the P_o. Because the modification rate of T1142C in Linsdell's study is >60-fold faster than that of ours, we measured the modification rate of T1142C in the presence of ATP plus pyrophosphate and found that the modification rate is not significantly different from that measured with ATP alone (Fig. S4). This result suggests that pyrophosphate is not likely the culprit behind the discrepancies between Linsdell's data and ours, which is perhaps not surprising because the P_o for most of the constructs in the presence of ATP alone is already ∼0.7 (e.g., Fig. 3). Fourth, whenever we deemed necessary, the reaction-induced current changes observed at the macroscopic

level were confirmed at the microscopic level in our study. These microscopic data not only serve to further confirm the reaction but also allow us to differentiate the consequences of reaction (alterations in channel open probability or conductance). Lastly, different expression systems were used (baby hamster kidney cells in their study vs. Chinese hamster ovary cells in ours). Setting aside these technical differences—some may be resolved by future standardization of the experimental protocol—we believe that our data showing high reactivity of cysteines on one face of TM12, reaction-induced changes in channel conductance, and strong blocker protection altogether lead to the conclusion that the cytoplasmic part of TM12 contributes to the formation of the chloride permeation pathway of CFTR.

Notwithstanding the aforementioned common components shared between the CFTR channel and ABC exporters, our data indicate that the overall shape of the permeation pathway in the CFTR channel differs significantly from that known for ABC exporters. In particular, in the ATP-bound outward-facing conformation of ABC exporters (Dawson and Locher, 2007; Ward et al., 2007), which is generally believed to represent the ATP-induced conducting (open) state of the CFTR channel (Vergani et al., 2005; Mense et al., 2006), the substrate translocation pathway accommodates a large cavity that is exposed to the extracellular solution but shielded from the cell interior (Fig. 7). However, several experimental observations suggest that the open state of CFTR harbors a funnel-shaped intracellular vestibule, with a wide intracellular entrance extending to a restricted region deep in the pore. First, reactivity toward intracellular MTS reagents is abundant at the inner half of TM12 but disappears at its external half (Fig. 1 C), consistent with a picture wherein a large intracellular vestibule connects to a restriction around the middle of the ion translocation pathway. Second, whereas cationic adducts at positions around the inner entrance enhance the single-channel current amplitude, both charged and uncharged adducts at a deeper position impede ion flow (Fig. 3). We interpret this result as the intracellular vestibule becomes progressively narrower along the ion-conducting pore. Finally, a funnel-shaped vestibule could also explain why a large pore blocker strongly protects sulfhydryls positioned deep in the pore against the modification but becomes less effective for the one at a more cytoplasmic position (Fig. 4 C).

The presence of a large intracellular vestibule in an open CFTR channel supports the degraded transporter hypothesis (Chen and Hwang, 2008; Jordan et al., 2008; Gadsby, 2009), which envisages that to allow rapid ion diffusion, the cytoplasmic barrier observed in the outward-facing conformation of ABC exporters has to be removed. On the other hand, if the ATP-free inward-facing conformation of ABC exporters represents a closed CFTR channel, the pore-lining residues are expected to also be accessible from the cytoplasmic side of the channel. Indeed, our data show significant reactivity in the absence of ATP at all positions that respond to $MTSES^-$ in the presence of ATP (Fig. 5 D). These results, collectively, suggest that the gate of CFTR is located at a more extracellular section of the pore. This proposition, however, appears to be in conflict with recent cysteine-scanning studies by Linsdell's group (El Hiani and Linsdell, 2010; Qian et al., 2011; Wang et al., 2011). They reported that access of intracellular sulfhydryl reagents to positions deep in the pore is state dependent, raising the possibility of the presence of a cytoplasmic gate. Because little state-dependent accessibility was observed for positions toward the cytoplasmic end of the channel pore, their results are not at odds with the degraded transporter hypothesis. Furthermore, it cannot be ruled out that the state-dependent reactivity is a result of other conformational changes. Indeed, our cysteine-scanning studies on TM6 (Bai et al., 2010) have provided evidence for a rotational movement based on the observation that $MTSET^+$ modification of three substituted cysteines that reside on one face of the TM6 α helix affects gating. Intriguingly, our present state-dependent accessibility data of TM12 is also consistent with the idea that this pore-lining TM rotates during channel gating (Fig. 5 D). The importance of this dynamic motion lies in the hypothesis, based on structural (Gutmann et al., 2010) and functional

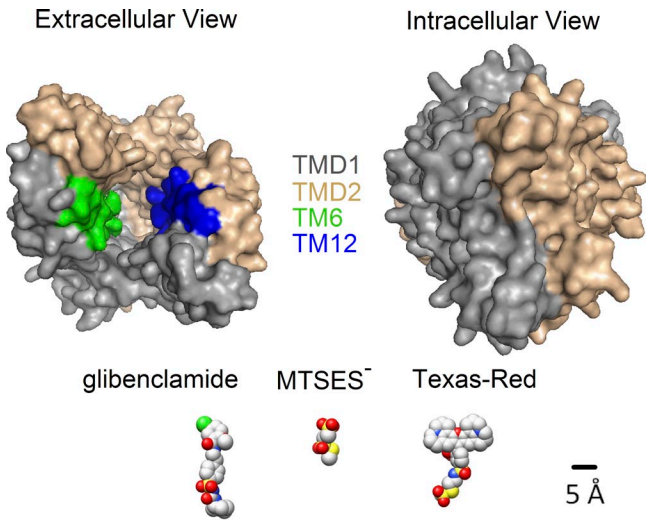

Figure 7. Surface representations of the TMDs (TMD1 and TMD2) of the ABC exporter SAV1866 (Protein Data Bank accession no. 2ONJ), viewed from the extracellular (left) or intracellular (right) side of the membrane. TMD1, TMD2, TM6, and TM12 are colored as indicated. On the same scale (black line), the blocker glibenclamide and two thiol reagents in their most extended configurations were shown for comparison. Note that the structure of the ABC protein shows an obliterated intracellular entrance, but our experimental data suggest that both glibenclamide and $MTSES^-$ can readily enter the CFTR pore from the intracellular side when the channel is in the open state.

(Rosenberg et al., 2001) studies of multidrug ABC exporters, that helical rotation of the TMs that form the substrate–translocation pathway converts a high-affinity substrate binding site to a low-affinity one and thereby facilitates substrate release, although future studies will be needed to establish whether this affinity change mechanism is common for all ABC exporters.

In addition to a rotational movement of the TMs, our results with Texas red $MTESA^+$ (Figs. 6 and 7; ~13 Å in diameter) demonstrate that closing of the CFTR channel expands the inner pore domain to allow Texas red $MTSEA^+$ to reach those residues lining the pore. At first glance, this idea seems counterintuitive because it implies that channel opening is associated with a narrowing of the cytoplasmic entrance. However, this tightening motion does not perturb chloride flow (an unhydrated chloride ion is ~3.6 Å in diameter) (Hille, 2001), as we show that the open channel is still wide enough to accommodate positively charged $MTSET^+$ adducts (Figs. 3 and 7; ~6 Å in diameter). Considering that positively charged residues at the cytoplasmic end are proposed to increase the concentrations of anions in the intracellular vestibule through an electrostatic mechanism (Aubin and Linsdell, 2006), one interesting possibility is that the tightening motion in the inner pore domain upon channel opening brings the positive charges closer to the ion permeation pathway to enhance this electrostatic effect. Additionally, the horizontal expansion/tightening at the cytoplasmic entrance during CFTR gating bears a resemblance to the flip-flop motion in ABC exporters when they switch between the outward- and inward-facing conformations. Overall, our data implicate that the gating structural dynamics of CFTR involves analogous conformational changes—helical rotation and horizontal expansion/tightening—that are associated with the transport cycle of ABC exporters, signifying a strong evolutionary relationship between these two functionally distinct proteins.

The boundary between ion channels and transporters has become blurred in light of emerging studies of members from each class (Gadsby, 2009; Miller and Nguitragool, 2009). Structural and functional work on CLC proteins (Dutzler et al., 2002, 2003; Accardi and Miller, 2004; Lísal and Maduke, 2008) have provided elegant evidence that similar mechanisms of gating and ion permeation are shared by CLC channels and transporters. Recent crystallographic data and kinetic modeling (Dutzler et al., 2003; Feng et al., 2010) on CLC transporters reveal a contiguous conduit that is expected to exist only in a channel, raising the possibility that the function of a CLC transporter can be realized by the presence of a kinetic barrier for channel-like diffusion and that removal of the barrier can turn a CLC transporter into a channel (Jayaram et al., 2008). Likewise, a recent report on the crystal structure of a K^+ transporter (Cao et al., 2011) reveals substantial structural similarity with K^+ channels (Doyle et al., 1998; Zhou et al., 2001). The overall shape of the selectivity filter, a fine-tuned structure that fulfills the task of selecting K^+ over Na^+, is strikingly conserved. Although the transport mechanism for this K^+ transporter is not identified, the slower ion transport rate relative to that expected from a K^+ channel is attributed to a physical barrier at the cytoplasmic end and a positively charged residue, as these structural features are absent in K^+ channels. Collectively, these reports lead to a common theme that the fundamental difference between channels and transporters, which exploit the conserved overall architecture to transport the same ion (e.g., Cl^- or K^+), lies in the absence or presence of a barrier for ion diffusion. The present work demonstrates that CFTR and ABC exporters, despite transporting immensely different cargos, also follow this common theme and thus provides a unique perspective on the evolutionary interconnection between ion channels and transporters.

We thank Dr. Kevin Gillis for critical reading of the manuscript and Cindy Chu for technical assistance.

This work was supported by National Institutes of Health (grants R01HL53445 and R01DK55835 to T.-C. Hwang).

Christopher Miller served as editor.

Submitted: 15 August 2011
Accepted: 12 October 2011

REFERENCES

Accardi, A., and C. Miller. 2004. Secondary active transport mediated by a prokaryotic homologue of ClC Cl− channels. *Nature.* 427:803–807. http://dx.doi.org/10.1038/nature02314

Alexander, C., A. Ivetac, X. Liu, Y. Norimatsu, J.R. Serrano, A. Landstrom, M. Sansom, and D.C. Dawson. 2009. Cystic fibrosis transmembrane conductance regulator: using differential reactivity toward channel-permeant and channel-impermeant thiol-reactive probes to test a molecular model for the pore. *Biochemistry.* 48:10078–10088. http://dx.doi.org/10.1021/bi901314c

Aller, S.G., J. Yu, A. Ward, Y. Weng, S. Chittaboina, R. Zhuo, P.M. Harrell, Y.T. Trinh, Q. Zhang, I.L. Urbatsch, and G. Chang. 2009. Structure of P-glycoprotein reveals a molecular basis for poly-specific drug binding. *Science.* 323:1718–1722. http://dx.doi.org/10.1126/science.1168750

Artigas, P., and D.C. Gadsby. 2003. Na+/K+-pump ligands modulate gating of palytoxin-induced ion channels. *Proc. Natl. Acad. Sci. USA.* 100:501–505. http://dx.doi.org/10.1073/pnas.0135849100

Aubin, C.N., and P. Linsdell. 2006. Positive charges at the intracellular mouth of the pore regulate anion conduction in the CFTR chloride channel. *J. Gen. Physiol.* 128:535–545. http://dx.doi.org/10.1085/jgp.200609516

Bai, Y., M. Li, and T.C. Hwang. 2010. Dual roles of the sixth transmembrane segment of the CFTR chloride channel in gating and permeation. *J. Gen. Physiol.* 136:293–309. http://dx.doi.org/10.1085/jgp.201010480

Bear, C.E., C.H. Li, N. Kartner, R.J. Bridges, T.J. Jensen, M. Ramjeesingh, and J.R. Riordan. 1992. Purification and functional reconstitution of the cystic fibrosis transmembrane conductance regulator (CFTR). *Cell.* 68:809–818. http://dx.doi.org/10.1016/0092-8674(92)90155-6

Cao, Y., X. Jin, H. Huang, M.G. Derebe, E.J. Levin, V. Kabaleeswaran, Y. Pan, M. Punta, J. Love, J. Weng, et al. 2011. Crystal structure of a potassium ion transporter, TrkH. *Nature.* 471:336–340. http://dx.doi.org/10.1038/nature09731

Chen, T.Y., and T.C. Hwang. 2008. CLC-0 and CFTR: chloride channels evolved from transporters. *Physiol. Rev.* 88:351–387. http://dx.doi.org/10.1152/physrev.00058.2006

Dawson, R.J., and K.P. Locher. 2006. Structure of a bacterial multidrug ABC transporter. *Nature.* 443:180–185. http://dx.doi.org/10.1038/nature05155

Dawson, R.J., and K.P. Locher. 2007. Structure of the multidrug ABC transporter Sav1866 from Staphylococcus aureus in complex with AMP-PNP. *FEBS Lett.* 581:935–938. http://dx.doi.org/10.1016/j.febslet.2007.01.073

Dawson, R.J., K. Hollenstein, and K.P. Locher. 2007. Uptake or extrusion: crystal structures of full ABC transporters suggest a common mechanism. *Mol. Microbiol.* 65:250–257. http://dx.doi.org/10.1111/j.1365-2958.2007.05792.x

Dean, M., and T. Annilo. 2005. Evolution of the ATP-binding cassette (ABC) transporter superfamily in vertebrates. *Annu. Rev. Genomics Hum. Genet.* 6:123–142. http://dx.doi.org/10.1146/annurev.genom.6.080604.162122

del Camino, D., and G. Yellen. 2001. Tight steric closure at the intracellular activation gate of a voltage-gated K(+) channel. *Neuron.* 32:649–656. http://dx.doi.org/10.1016/S0896-6273(01)00487-1

del Camino, D., M. Holmgren, Y. Liu, and G. Yellen. 2000. Blocker protection in the pore of a voltage-gated K+ channel and its structural implications. *Nature.* 403:321–325. http://dx.doi.org/10.1038/35002099

Doyle, D.A., J. Morais Cabral, R.A. Pfuetzner, A. Kuo, J.M. Gulbis, S.L. Cohen, B.T. Chait, and R. MacKinnon. 1998. The structure of the potassium channel: molecular basis of K+ conduction and selectivity. *Science.* 280:69–77. http://dx.doi.org/10.1126/science.280.5360.69

Dutzler, R., E.B. Campbell, M. Cadene, B.T. Chait, and R. MacKinnon. 2002. X-ray structure of a ClC chloride channel at 3.0 A reveals the molecular basis of anion selectivity. *Nature.* 415:287–294. http://dx.doi.org/10.1038/415287a

Dutzler, R., E.B. Campbell, and R. MacKinnon. 2003. Gating the selectivity filter in ClC chloride channels. *Science.* 300:108–112. http://dx.doi.org/10.1126/science.1082708

El Hiani, Y., and P. Linsdell. 2010. Changes in accessibility of cytoplasmic substances to the pore associated with activation of the cystic fibrosis transmembrane conductance regulator chloride channel. *J. Biol. Chem.* 285:32126–32140. http://dx.doi.org/10.1074/jbc.M110.113332

Feng, L., E.B. Campbell, Y. Hsiung, and R. MacKinnon. 2010. Structure of a eukaryotic CLC transporter defines an intermediate state in the transport cycle. *Science.* 330:635–641. http://dx.doi.org/10.1126/science.1195230

Gadsby, D.C. 2009. Ion channels versus ion pumps: the principal difference, in principle. *Nat. Rev. Mol. Cell Biol.* 10:344–352. http://dx.doi.org/10.1038/nrm2668

Gutmann, D.A., A. Ward, I.L. Urbatsch, G. Chang, and H.W. van Veen. 2010. Understanding polyspecificity of multidrug ABC transporters: closing in on the gaps in ABCB1. *Trends Biochem. Sci.* 35:36–42. http://dx.doi.org/10.1016/j.tibs.2009.07.009

Hille, B. 2001. Ion Channels of Excitable Membranes. Third edition. Sinauer, Sunderland, MA. 814 pp.

Hollenstein, K., R.J. Dawson, and K.P. Locher. 2007. Structure and mechanism of ABC transporter proteins. *Curr. Opin. Struct. Biol.* 17:412–418. http://dx.doi.org/10.1016/j.sbi.2007.07.003

Jardetzky, O. 1966. Simple allosteric model for membrane pumps. *Nature.* 211:969–970. http://dx.doi.org/10.1038/211969a0

Jayaram, H., A. Accardi, F. Wu, C. Williams, and C. Miller. 2008. Ion permeation through a Cl−-selective channel designed from a CLC Cl−/H+ exchanger. *Proc. Natl. Acad. Sci. USA.* 105:11194–11199. http://dx.doi.org/10.1073/pnas.0804503105

Johnson, J.P., Jr., and W.N. Zagotta. 2005. The carboxyl-terminal region of cyclic nucleotide-modulated channels is a gating ring, not a permeation path. *Proc. Natl. Acad. Sci. USA.* 102:2742–2747. http://dx.doi.org/10.1073/pnas.0408323102

Jordan, I.K., K.C. Kota, G. Cui, C.H. Thompson, and N.A. McCarty. 2008. Evolutionary and functional divergence between the cystic fibrosis transmembrane conductance regulator and related ATP-binding cassette transporters. *Proc. Natl. Acad. Sci. USA.* 105:18865–18870. http://dx.doi.org/10.1073/pnas.0806306105

Karlin, A., and M.H. Akabas. 1998. Substituted-cysteine accessibility method. *Methods Enzymol.* 293:123–145. http://dx.doi.org/10.1016/S0076-6879(98)93011-7

Khare, D., M.L. Oldham, C. Orelle, A.L. Davidson, and J. Chen. 2009. Alternating access in maltose transporter mediated by rigid-body rotations. *Mol. Cell.* 33:528–536. http://dx.doi.org/10.1016/j.molcel.2009.01.035

Larsson, H.P., O.S. Baker, D.S. Dhillon, and E.Y. Isacoff. 1996. Transmembrane movement of the shaker K+ channel S4. *Neuron.* 16:387–397. http://dx.doi.org/10.1016/S0896-6273(00)80056-2

Li, M., T. Kawate, S.D. Silberberg, and K.J. Swartz. 2010. Pore-opening mechanism in trimeric P2X receptor channels. *Nat Commun.* 1:44.

Lísal, J., and M. Maduke. 2008. The ClC-0 chloride channel is a 'broken' Cl−/H+ antiporter. *Nat. Struct. Mol. Biol.* 15:805–810. http://dx.doi.org/10.1038/nsmb.1466

Liu, Y., M. Holmgren, M.E. Jurman, and G. Yellen. 1997. Gated access to the pore of a voltage-dependent K+ channel. *Neuron.* 19:175–184. http://dx.doi.org/10.1016/S0896-6273(00)80357-8

Loo, T.W., and D.M. Clarke. 1997. Identification of residues in the drug-binding site of human P-glycoprotein using a thiol-reactive substrate. *J. Biol. Chem.* 272:31945–31948. http://dx.doi.org/10.1074/jbc.272.51.31945

McDonough, S., N. Davidson, H.A. Lester, and N.A. McCarty. 1994. Novel pore-lining residues in CFTR that govern permeation and open-channel block. *Neuron.* 13:623–634. http://dx.doi.org/10.1016/0896-6273(94)90030-2

Mense, M., P. Vergani, D.M. White, G. Altberg, A.C. Nairn, and D.C. Gadsby. 2006. In vivo phosphorylation of CFTR promotes formation of a nucleotide-binding domain heterodimer. *EMBO J.* 25:4728–4739. http://dx.doi.org/10.1038/sj.emboj.7601373

Miller, C., and W. Nguitragool. 2009. A provisional transport mechanism for a chloride channel-type Cl−/H+ exchanger. *Philos. Trans. R. Soc. Lond. B Biol. Sci.* 364:175–180. http://dx.doi.org/10.1098/rstb.2008.0138

Oldham, M.L., A.L. Davidson, and J. Chen. 2008. Structural insights into ABC transporter mechanism. *Curr. Opin. Struct. Biol.* 18:726–733. http://dx.doi.org/10.1016/j.sbi.2008.09.007

Paumi, C.M., M. Chuk, J. Snider, I. Stagljar, and S. Michaelis. 2009. ABC transporters in Saccharomyces cerevisiae and their interactors: new technology advances the biology of the ABCC (MRP) subfamily. *Microbiol. Mol. Biol. Rev.* 73:577–593. http://dx.doi.org/10.1128/MMBR.00020-09

Qian, F., Y. El Hiani, and P. Linsdell. 2011. Functional arrangement of the 12th transmembrane region in the CFTR chloride channel pore based on functional investigation of a cysteine-less CFTR variant. *Pflugers Arch.* 462:559–571.

Rees, D.C., E. Johnson, and O. Lewinson. 2009. ABC transporters: the power to change. *Nat. Rev. Mol. Cell Biol.* 10:218–227. http://dx.doi.org/10.1038/nrm2646

Riordan, J.R., J.M. Rommens, B. Kerem, N. Alon, R. Rozmahel, Z. Grzelczak, J. Zielenski, S. Lok, N. Plavsic, J.L. Chou, et al. 1989. Identification of the cystic fibrosis gene: cloning and characterization

of complementary DNA. *Science*. 245:1066–1073. http://dx.doi.org/10.1126/science.2475911

Rosenberg, M.F., G. Velarde, R.C. Ford, C. Martin, G. Berridge, I.D. Kerr, R. Callaghan, A. Schmidlin, C. Wooding, K.J. Linton, and C.F. Higgins. 2001. Repacking of the transmembrane domains of P-glycoprotein during the transport ATPase cycle. *EMBO J.* 20:5615–5625. http://dx.doi.org/10.1093/emboj/20.20.5615

Sheppard, D.N., and K.A. Robinson. 1997. Mechanism of glibenclamide inhibition of cystic fibrosis transmembrane conductance regulator Cl− channels expressed in a murine cell line. *J. Physiol.* 503:333–346. http://dx.doi.org/10.1111/j.1469-7793.1997.333bh.x

Sheppard, D.N., and M.J. Welsh. 1999. Structure and function of the CFTR chloride channel. *Physiol. Rev.* 79:S23–S45.

Smith, S.S., X. Liu, Z.R. Zhang, F. Sun, T.E. Kriewall, N.A. McCarty, and D.C. Dawson. 2001. CFTR: Covalent and noncovalent modification suggests a role for fixed charges in anion conduction. *J. Gen. Physiol.* 118:407–431. http://dx.doi.org/10.1085/jgp.118.4.407

Vergani, P., S.W. Lockless, A.C. Nairn, and D.C. Gadsby. 2005. CFTR channel opening by ATP-driven tight dimerization of its nucleotide-binding domains. *Nature*. 433:876–880. http://dx.doi.org/10.1038/nature03313

Wang, W., Y. El Hiani, and P. Linsdell. 2011. Alignment of transmembrane regions in the cystic fibrosis transmembrane conductance regulator chloride channel pore. *J. Gen. Physiol.* 138:165–178.

Ward, A., C.L. Reyes, J. Yu, C.B. Roth, and G. Chang. 2007. Flexibility in the ABC transporter MsbA: Alternating access with a twist. *Proc. Natl. Acad. Sci. USA*. 104:19005–19010. http://dx.doi.org/10.1073/pnas.0709388104

Zhou, Y., J.H. Morais-Cabral, A. Kaufman, and R. MacKinnon. 2001. Chemistry of ion coordination and hydration revealed by a K+ channel-Fab complex at 2.0 A resolution. *Nature*. 414:43–48. http://dx.doi.org/10.1038/35102009

Zhou, Z., S. Hu, and T.C. Hwang. 2002. Probing an open CFTR pore with organic anion blockers. *J. Gen. Physiol.* 120:647–662. http://dx.doi.org/10.1085/jgp.20028685